Voltage-induced long-range coherent electron transfer through organic molecules – Supplementary Information

K. Michaeli,[a] D.N. Beratan,[b,c,d] D.H. Waldeck,[e] R. Naaman[f]

a. Department of Condensed Matter Physics, Weizmann Institute of Science, Rehovot 76100 Israel

b. Department of Chemistry, Duke University, Durham, NC 27708 USA

c. Department of Physics, Duke University, Durham, NC 27708 USA

d. Department of Biochemistry, Duke University, Durham, NC 27710 USA

e. Chemistry Department, University of Pittsburgh, Pittsburgh PA 15260 USA

f. Department of Chemical and Biological Physics, Weizmann Institute of Science, Rehovot 76100 Israel

Density of states and localization length of the molecular bridge model

The molecular bridge model with a single state per site, given by Eq. 1 of the main text, is used in our work to demonstrate the effect of an applied electric field on electron transport through organic molecules. In this section, we present two properties of the molecular bridge in the absence of electric field: (i) the density of states (DOS) and (ii) the localization length. We start with a perfectly periodic bridge with uniform on-site energies $\varepsilon_n = \varepsilon$ and inter-site couplings $t_n = t$

$$H = -\sum_{n=1}^{N-1} t\left(c_{n+1}^{\dagger} c_n + c_n^{\dagger} c_{n+1} \right) + \sum_{n=1}^{N} \varepsilon\, c_n^{\dagger} c_n. \qquad \text{(SI1)}$$

An illustration of the model and the calculated DOS (for $\varepsilon = 2t$) are plotted in Figure SI1(a). To eliminate finite-size effects, we have calculated the DOS for a long bridge with $N = 1000$ sites. All electronic states corresponding to the above Hamiltonian are extended, i.e., their localization length is infinite, and a metallic band is formed at energies $\varepsilon - 2t < E < \varepsilon + 2t$.

Upon introducing a disorder potential to the model

www.pnas.org/cgi/doi/10.1073/pnas.1816956116

$$H = -\sum_{n=1}^{N-1} t\left(c_{n+1}^{\dagger} c_n + c_n^{\dagger} c_{n+1} \right) + \sum_{n=1}^{N} [\varepsilon + U_{\text{dis}}(n)] c_n^{\dagger} c_n, \qquad \text{(SI2)}$$

all the electronic states become localized. This model as well as the corresponding DOS and localization length are shown in Figure SI1(b). Here (as in the main text) we considered uniformly distributed uniformly distributed disorder, $U_{\text{dis}}(n) \in [-W, W]$ with $W = t$. As a result of the disorder, the band of electronic states extends over a window of energy $\varepsilon - 2t - W \lesssim E \lesssim \varepsilon + 2t + W$, which is wider in comparison to the periodic case. Crucially, the electronic wave functions decay exponentially with distance, $\Psi(n) \sim e^{-n\, d_0/\ell_{\text{loc}}(E)}$, where the energy dependence of the localization length $\ell_{\text{loc}}(E)$ is plotted in Figure SI1(b). Specifically, $\ell_{\text{loc}}(E)$ grows with energy in the lower half of the band and decreases in the upper half, i.e., the wave function becomes less localized as the system approaches the middle of the band. If the largest localization length at any energy is smaller than the length of the molecule, the electron transmission probability through the system is *always* exponentially small $\mathrm{T}(L) \sim e^{-2L/\ell_{\text{loc}}(E)}$.

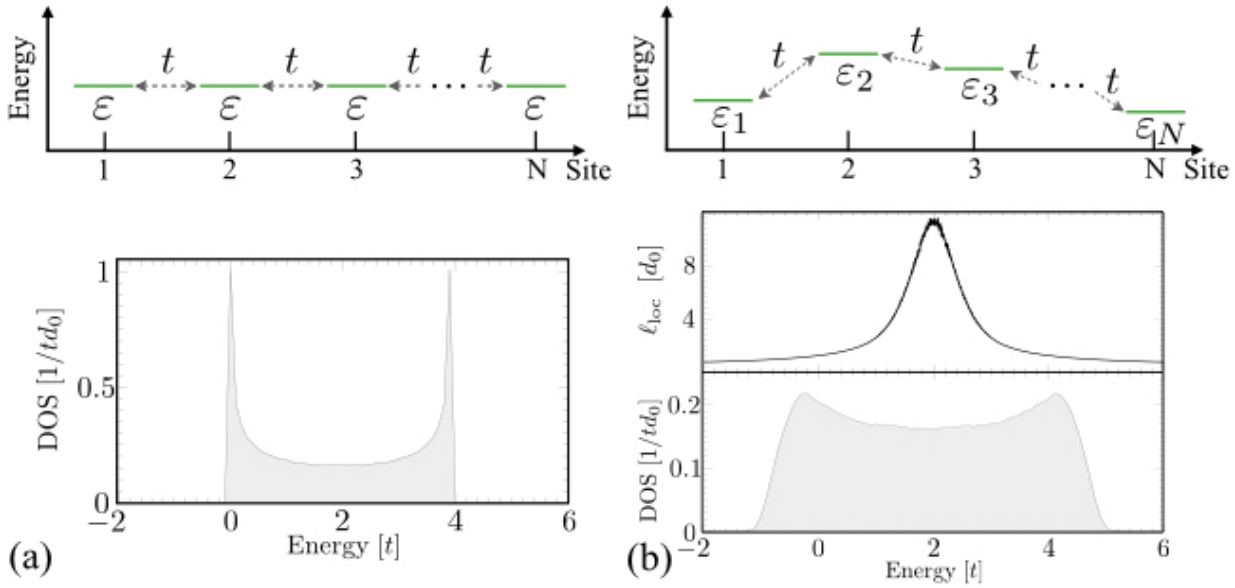

Figure SI1: Panel (a) shows a chain of N identical sites (top), and the corresponding density-of-stats (DOS) for the band of extended states which is formed over the interval $0 < E < 4t$ (bottom). Here, and throughout the paper, we take $\varepsilon = 2t$. Panel (b) shows a disordered chain in which the on-site energies are uniformly distributed in the interval $[-t, t]$. The corresponding DOS, which is plotted below, extends over a larger range of energies. As explained in the text, the localization length (ℓ_{loc}), which is plotted above the DOS, grows as energy increases (decreases) in the lower (upper) half of the band.

Survey of experiments that observe weakly temperature-dependent long-range transport

A number of electron transport measurements in metal-molecule-metal junctions, with bridges extending 5 nm, report weak temperature dependences [S1-S6]. For example, McCreery and co-workers [S1,S2] studied the voltage and temperature dependence of charge transport through ultrathin layers (4 nm to 22 nm) of conjugated organic molecules (e.g., fluorene anthraquinone, azobenzene, and bis-thienylbenzene). They found that the conductance changes by less than a factor of two over a temperature range of 200 K to 440 K. At temperatures below 100 K the transport appears to be non-activated. Nichols *et al.* [S4] examined the molecular conductance of 15-mer DNA duplexes [both $(AT)_{15}$ and $(GC)_{15}$ of about 5 nm in length] as a function of temperature from 290 K to 350 K with STM break junction methods and found temperature independent transport. The conductance of the AT- is 2-3 times lower than that of the GC duplex. The weak temperature dependence reported in these experiments is inconsistent with the temperature dependence that is expected for a multistep hopping mechanism with an activation free energy of about 0.2 – 0.5 eV, typical of molecular junction measurements on conjugated polymers [S7,S8]. It is challenging to understand rapid transport over these distances in the conventional theoretical framework, as the activation free energies would not allow rapid charge transport.

A number of studies that analyzed bridges of different lengths have shown a transition from direct superexchange (single-step tunneling with rates that drop exponentially with distance) to a power law distance dependence [S4,S6,S9,S10] around a few nanometers (< 4nm). A multi-step incoherent hopping transport mechanism rationalizes the power-law length dependence (i.e., the carrier diffuses on the bridge). In this regime, thermal activation arises because of the activation free energy required to inject carriers onto the bridge and the activation free energy for site-to-site hopping [S7,S8], or in electrochemical junctions by reorganization energy of the redox couple [S11,S12]. McCreery *et al.* [S1,S2] and Porath *et al.* [S13] reported voltage dependences for the current in molecular junctions, which are attributed to lowering of the barrier and screening of the applied field by the molecules. This explanation assumes that the electronic states above the barrier are all extended. In most organic molecules, however, the states directly above the barrier are localized while extended states can only be found at much higher energies. Our theory, which accounts for the change in nature of the electronic states from localized to quasi-extended, also includes the change in the barrier height.

Outline of the numerical calculation

The results given in the main text for the electron transmission probability and current through the molecules were obtained using two different numerical methods: (i) For the analysis of the single-band Hamiltonian (Eq. 1) we followed the numerical method of Ref. S14, which is based on the Poincaré map representation of the Schrödinger equation and is commonly known as the transfer matrix method. (ii) The transmission probability through DNA molecules modeled by the multi-band Hamiltonian in Eq. 5 was obtained by numerical computation of the Green's function. Below, we outline both methods.

Calculation of the transmission probability for the single-band model:

The aim of the numerical derivation is to find transmission probability for each realization of the disorder potential $U_{\text{dis}}(n)$, and then average it over a large number of realizations. In practice, we average the logarithm of the transmission probability, which is more stable and leads to faster convergence [S15].

The first step in the derivation is to write a continuum version of the Schrödinger equation corresponding to Eq. 1, with $t_n = t$ and $\varepsilon_n = \varepsilon + U_{\text{dis}}(n)$,

$$E\psi(x) = -td_0^2 \frac{\partial^2 \psi(x)}{\partial x^2} + \sum_{n=1}^{N} [\varepsilon - 2t + U_{\text{dis}}(n) + \mathcal{V}_n]\, \psi(x)\delta(x - nd_0), \qquad \text{(SI3)}$$

where $\psi(x)$ is the electronic wave function. This continuum version of the Schrödinger equation coincides with the discrete one for electrons transmitted with energies near the bottom (top) of the electronic band, i.e., $\varepsilon - 2t < E \ll \varepsilon$ or $\varepsilon \ll E < \varepsilon + 2t$. The second numerical method, which is introduced below, is better suited for giving accurate results at arbitrary energy of the transmitted electron. However, the second method is significantly slower, and thus, limits the size of the system and the number of disorder realizations over which we can average.

Between two neighboring sites, $(n-1)d_0 < x < nd_0$, the solution for the above equation can be written as [S16]

$$\psi(x) = A_n e^{-ix\sqrt{(E-\varepsilon+2t-\mathcal{V}_n)/td_0^2}} + B_n e^{ix\sqrt{(E-\varepsilon+2t-\mathcal{V}_n)/td_0^2}}, \tag{SI4}$$

with the boundary conditions:

$$\lim_{\epsilon\to 0}[\psi(x+\epsilon) - \psi(x-\epsilon)] = 0; \tag{SI5a}$$

$$\lim_{\epsilon\to 0} td_0\left[\frac{d\psi(x+\epsilon)}{dx} - \frac{d\psi(x-\epsilon)}{dx}\right] = U_{\text{dis}}(n)\psi(x). \tag{SI5b}$$

This representation of the solution is meaningful only if $E - \varepsilon + 2t - \mathcal{V}_n > 0$ for all n, i.e., for energies within the electronic band. For simplicity, we set $\varepsilon = 2t$ below, as we did in the main text.

Combining Eqs. SI4 and SI5 results in a recursive relation for the wave function at position $(n+1)d_0$

$$\psi(n+1) = \left[\cos\sqrt{E-\mathcal{V}_{n+1}} + \frac{\sqrt{E-\mathcal{V}_n}\sin\sqrt{E-\mathcal{V}_{n+1}}}{\sqrt{E-\mathcal{V}_{n+1}}\sin\sqrt{E-\mathcal{V}_n}}\cos\sqrt{E-\mathcal{V}_n} + U_{\text{dis}}(n)\frac{\sin\sqrt{E-\mathcal{V}_{n+1}}}{\sqrt{E-\mathcal{V}_{n+1}}}\right]\psi(n) - \frac{\sin\sqrt{E-\mathcal{V}_{n+1}}}{\sqrt{E-\mathcal{V}_{n+1}}}\psi(n-1). \tag{SI6}$$

The boundary conditions for the scattering problem need to be set, in order to find the corresponding transmission probability. We adopt the convention that the molecule is located between sites 3 and $N+2$, while the electrodes connected to it are found at sites $n < 3$ and $n > N+2$. In other words, $\varepsilon,\ U_{\text{dis}}(n),\ \mathcal{V}_n \neq 0$ only for $3 \le n \le N+2$, and the wave function at the electrodes can be written as

$$\psi(n) = \begin{cases} e^{-in\sqrt{E/t}} & n \le 2 \\ \vartheta^{-1}e^{-in\sqrt{(E-eV)/t}} + \rho\vartheta^{-1}e^{in\sqrt{(E-eV)/t}}. & n \ge N+2 \end{cases}, \tag{SI7}$$

Here, ρ and ϑ are the reflection and transmission amplitudes for an electron scattered by the molecule. By inserting the boundary conditions $\psi(1) = e^{-i\sqrt{E/t}}$ and $\psi(2) = e^{-2i\sqrt{E/t}}$ into

Eq. SI6, we numerically calculate $\psi(N+2)$ and $\psi(N+3)$, and extract ϑ as well as the corresponding transmission probability

$$T = \sqrt{\frac{E}{E-V}}|\vartheta|^2 = \sqrt{\frac{E}{E-eV}}\left|\frac{1-e^{2i\sqrt{(E-eV)/t}}}{\psi(n+3)-e^{i\sqrt{(E-eV)/t}}\psi(n+2)}\right|^2 \qquad \text{(SI8)}$$

Calculation of the transmission probability for the multi-band model:

In the second numerical method, we keep the discrete form of the Schrödinger equation corresponding to the Hamiltonian in Eq. 5 for -$\infty < n < \infty$

$$\begin{aligned} E\psi_i(n) = &-\sum_{j=0}^{\infty}\left[t_{i,j}(n,n+1)\psi_j(n+1)+t_{i,j}(n,n-1)\psi_j(n-1)\right] \qquad \text{(SI9)} \\ &+[\varepsilon_i(n)-2t_i(n)+U_{\mathrm{dis}}(n)+\mathcal{V}(n)]\psi_i(n), \end{aligned}$$

where $t_{i,j}(n,m) = t_{i,j}(m,n) = t_{j,i}(n,m) = t_{j,i}(m,n)$ and t_i is the average coupling between electrons in state i on neighboring sites. For a molecule of length $N \equiv \frac{L}{d_0}$ coupled from both sides to electrodes $\varepsilon_i(n), U_{\mathrm{dis}}(n) \neq 0$ only for $1 \leq n \leq N$, and $\mathcal{V}(n) = 0$ for $n \leq 0$ and $\mathcal{V}(n) = V$ for $n \geq N$. Moreover, we model the electrodes as one-dimensional wires with the same number of bands as electronic states per site. The couplings between neighboring sites in the electrodes are taken to be uniform and do not mix different bands $t_{i,j}(n,n+1) = t_{i,j}(n,n-1) = t_0\delta_{i,j}$ for $n < -1$ and $n > N+1$. Each band in the left (right) electrode is coupled to a single state on the $n = 0$ ($n = N$) site, i.e.,

$$t_{i,j}(0,1) = t_{i,j}(N,N+1) = t\delta_{i,j}. \qquad \text{(SI10)}$$

For simplicity, we have taken the coupling to the electrodes to be equal to the average coupling in the molecule. Changing the coupling in Eq. SI10 quantitively modifies the transmission probability through the molecule, but keeps its scaling with the voltage the same.

To reduce the infinite set of Schrödinger equations described by Eq. SI9 to a finite one, we focus only on the relevant electronic states $i = 0 \ldots M-1$ (in our calculations $M = 5$). In addition, we

describe the electronic states inside the electrode using the scattering states for electrons transmitted through the molecule from the left to the right electrodes

$$\psi_i(n<0) = \sqrt{\frac{1}{M}} e^{in\sqrt{E/t_0}} + \sum_{j=0}^{M-1} \rho_{i,j} e^{-in\sqrt{E/t_0}}; \tag{SI11a}$$

$$\psi_i(n>N) = \sum_{j=0}^{M-1} \vartheta_{i,j} e^{in\sqrt{(E-V)/t_0}}. \tag{SI11b}$$

Here $\rho_{i,j}$ and $\vartheta_{i,j}$ are the reflection and transmission amplitudes for an electron with energy E which starts in the ith band of the lead and ends in the jth band. Similar scattering wave-functions can be written for electrons transmitted in the opposite direction. Following Ref. S17, we use continuity of the wave-function at $n = 0$ and $n = N$ to write the set of coupled Schrödinger equations for $0 \le n \le N$

$$\begin{aligned} S_i(n)\psi_i(n) = &-\sum_{j=0}^{\infty}\left[t_{i,j}(n,n+1)\psi_j(n+1) + t_{i,j}(n,n-1)\psi_j(n-1)\right] \\ &+ [\varepsilon_i(n) - 2t_i(n) + U_{\mathrm{dis}}(n) + \mathcal{V}(n) - E - \Sigma_i(n)]\psi_i(n), \end{aligned} \tag{SI12}$$

where $\Sigma_i(n) = e^{i\sqrt{E/t_0}}$, $S_i(n) = -\frac{2i}{\sqrt{M}} \sin\sqrt{E/t_0}\, \delta_{n,0}$, and the total transmission probability is $T = \sum_i |\psi_i(N)|^2$. Thus, to find the transmission probability we numerically solve the set of equations (Eq. SI12) for $\psi_i(N)$.

Effect of screening on the voltage-induced long-range electron transfer mechanism

In the main text we explored only the effect of a uniform electric field, i.e., assumed the voltage drop is constant along the molecule and there are no screening effects. Clearly, screening can significantly alter the ability of the electric field to mix states with different localization length. In particular, it becomes less effective as the electric field decreases. Nevertheless, the conclusions do not qualitatively change as long as the local electric field is non-zero over a length larger than $\ell_{\mathrm{loc}}(E)$. In Figure SI2(a) we present a numerical calculation of the electron transmission probability as a function of length for $eV = 1t$ with three different potential profiles:

(i) Linear drop (uniform electric field) $\mathcal{V}_n = -eV(1 - n/L)$.

(ii) Power-law screened potential $\mathcal{V}_n = -eV[(n\, d_0/\lambda)^2 + 1]^{-k/2}$ with $k = 2$ and $\lambda = 4$.

(iii) Exponential screening $\mathcal{V}_n = -eVe^{-n\, d_0/\lambda}$ with $\lambda = 2$.

We find that the slope obtained from a plot of the transmission coefficient versus the length (for a fixed voltage) grows as screening effects becomes more significant. To estimate the dependence of the transmission on length and voltage, we calculate $\Psi(n = N)$ using the same strategies that led to Eq. 2 in the main text. For a potential along the molecule of the form $\mathcal{V}_n = -eV\, f(nd_0/\lambda)$, where $f(z)$ is a monotonic function and λ sets the length scale at which screening effect becomes important, Eq. 2 becomes

$$\Psi(N) \sim \exp\left\{-\sum_{m=1}^{N} \frac{\mathrm{d}_0}{\ell_{\mathrm{loc}}\big(E(m)\big)}\right\} \sim \exp\left\{-\frac{U}{td_0}\sum_{m=1}^{N} \frac{1}{E + eV\, f(nd_0/\lambda)}\right\}. \qquad \text{(SI13)}$$

In the limit $|eV| \gg E$, the transmission probability decays as a function of L with a characteristic length that is larger than $\ell_{\mathrm{loc}}(E)$. The length $\bar{\ell}$, however, no longer scales linearly with the voltage. For example, it is proportional to $|V|^{1/k}$ when $f(z) = z^{-k}$ [see Figure SI2(b)].

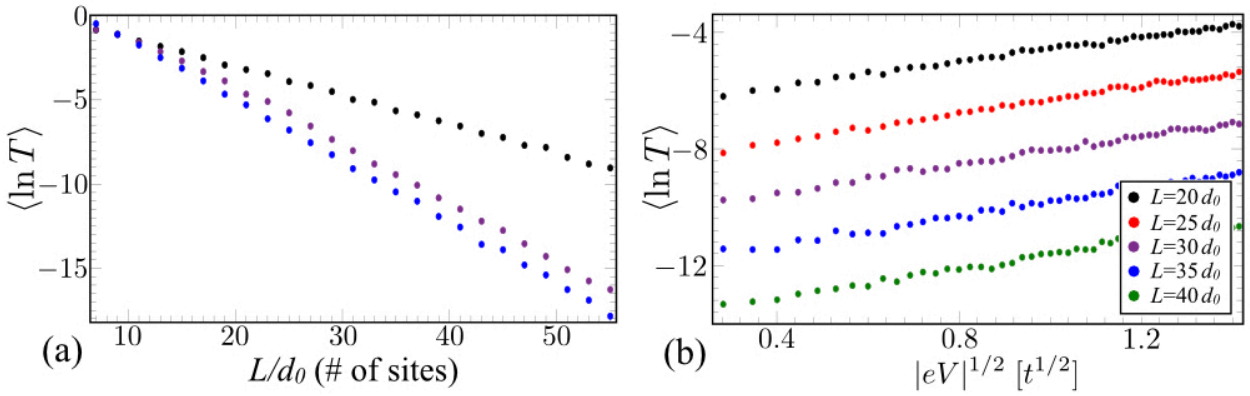

Figure SI2: The disorder averaged logarithm of the transmission probability at $E = 0.05$ is plotted as a function of length (panel a) and voltage (panel b) for a non-linear form of the electric potential. The transmission in panel (a) is calculated for $\mathcal{V}_n = -eV[(n/4)^2 + 1]^{-1}$ (purple) and $\mathcal{V}_n = -eV \cdot \exp(-n/2)$ (blue) in comparison to a linear drop$\mathcal{V}_n = -eV(1 - n/L)$ (black), with $eV = t$. To compare the slopes of all three curves we shifted them so that they all coincide at $L = 9d_0$. Although the largest effect occurs for constant $\mathcal{E}$, it is still significant as long as the electric field is non-zero throughout the molecule. The voltage dependence of the transmission for the potential $\mathcal{V}_n = -eV[(n/4)^2 + 1]^{-1}$is shown in panel (b). The characteristic decay length of the transmission is proportional to $V^{1/2}$.

Connection to the experimental finding of Refs. S1-S3

Of the several papers reporting weak temperature dependence of charge transfer through organic molecules, only a few have systematically studied the voltage dependence [S1-S3]. In Refs. S1-S2, it was found that the logarithm of the electric current through different organic semiconductors of different length scales as $|V|^{1/2}$. Rough estimates of the low-temperature current-voltage curves for charge transfer through peptides (figure 3 of Ref. S3), reveals that $\ln(I) \sim |V|^{-p}$ with $p \approx 1$. The calculation of the current as a function of voltage shown in the main text (Figure 4) can explain the result of Ref. S3 but not of Refs. S1-S2.

In the previous section of the SI we studied how screening affects the electric-field induced (quasi-) delocalization mechanism. Specifically, we showed that power-law screening give rise to transmission of the form $\ln T \sim |V|^{1/k}$. Calculation of the current using the Landauer formula (see Eq. 4 of the main text and the discussion in its vicinity), shows that a screened potential of the form $\mathcal{V}_n = -eV[(n/4)^2 + 1]^{-k/2}$ with $k = 2$ may explain the result of Refs. S1-S2. The result of the calculation for different values of the chemical potential in the right lead, $\mu_R - (\varepsilon - 2t)$, is presented in Figure SI3. We note that in all our derivations $\varepsilon - 2t$ was set to be zero by a trivial shift in the total energy. The inset shows that the scaling $\ln(I) \sim |V|^{1/2}$ becomes better as the chemical potential of the leads is closer to the energy of the bridge.

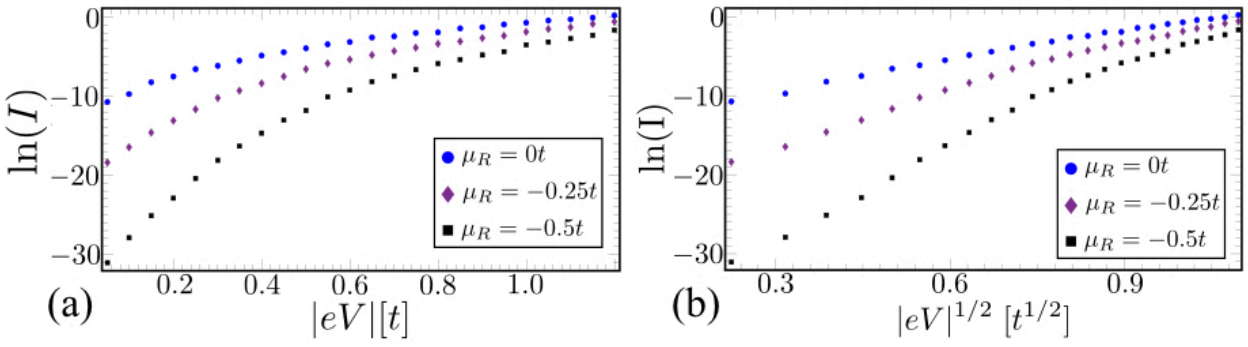

Figure SI3: The current as a function of voltage for different chemical potentials in the right contacts [panel (a)] for a molecule of length $L = 30d_0$. Panel (b) demonstrates the scaling of the logarithm of the current with $V^{1/2}$. This scaling becomes better as the chemical potential of the right lead approaches the bridge energy.

Current-voltage characteristics for the DNA model

In the main text we demonstrated that the effect of an applied electric field on a realistic model for a DNA bridge molecule is qualitatively the same as for the simple bridge given by Eq. 1 of the main text. For this purpose, we introduced a bridge with several orbital states per-site (Eq. 5 of the main text), which represent the various HOMO levels of the nucleic acids. There, we also calculated the length dependence of the transmission for different values of the electric field. For completeness, we show in Figure SI4 the current as function of voltage for molecules of different lengths and for different values of μ_R. The calculation was performed for the same parameters as in the main text. Please note the similarity between Figure SI4(a) and Figure 4 of the main text.

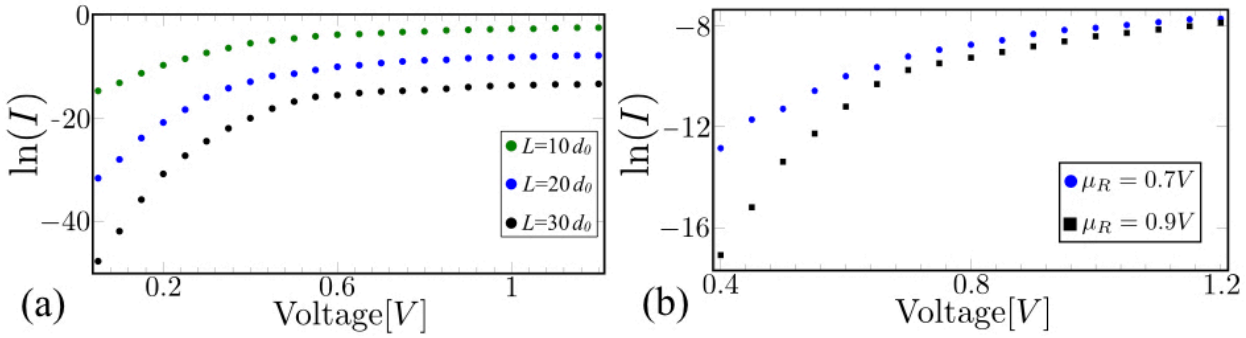

Figure SI4: The current as a function of voltage for molecules of various lengths [panel (a)], and for different chemical potentials in the right contacts [panel (b)]. The chemical potential in panel (a) was taken to be $\mu_R = 0.7$, and the length of the molecule in panel (b) is $L = 30d_0$ The inset shows that the current grows exponentially with the voltage as $\ln(I) \sim V^{-1}$ at high voltage.

References:

[S1] H. Yan, A. J. Bergren, R. McCreery, M. L. D. Rocca, P. Martin, P. Lafarge, J. Christophe Lacroix, Activationless charge transport across 4.5 to 22 nm in molecular electronic junctions, PNAS, 110, 5326–5330 (2013).

[S2] A. M. Najarian, R. L. McCreery, Structure Controlled Long-Range Sequential Tunneling in Carbon-Based Molecular Junctions, ACS Nano 11, 3542−3552. (2017).

[S3] C. D. Bostick, S. Mukhopadhyay, I. Pecht, M. Sheves, D. Cahen and D. Lederman, Protein bioelectronics: a review of what we do and do not know, *Rep. Prog. Phys.* 81, 026601 (2018).

[S4] H. van Zalinge, D. J. Schiffrin, A. D. Bates, E. B. Starikov, W. Wenzel, and R. J. Nichols, Variable-Temperature Measurements of the Single-Molecule Conductance of Double-Stranded DNA. *Angew. Chem. Int. Ed.*, 45, 5499-5502 (2006).

[S5] L. Sepunaru, S. Refaely-Abramson, R. Lovrincic, Y. Gavrilov, P. Agrawal, Y. Levy, L. Kronik, I. Pecht, M. Sheves, Mordechai, and D. Cahen, Electronic Transport via Homopeptides: The Role of Side Chains and Secondary Structure, *J. Am. Chem. Soc.* 137, 9617–9626 (2015).
[S6] L. Sepunaru, I. Pecht, M. Sheves, and D. Cahen, Solid-State Electron Transport across Azurin: From a Temperature-Independent to a Temperature-Activated Mechanism, *J. Am. Chem. Soc.* 133*,* 2421–2423 (2011).
[S7] S.H. Choi, B. Kim, C. D. Frisbie, Electrical Resistance of Long Conjugated Molecular Wires, *Science* 320, 1482-1486 (2008).
[S8] T. Hines, I. Diez-Perez, J. Hihath,H. Liu, Z.-S. Wang, J. Zhao, G. Zhou, K. Muellen, and N. J. Tao, Transition from Tunneling to Hopping in Single Molecular Junctions by Measuring Length and Temperature Dependence*, J. Am. Chem. Soc*. 132, 11658–11664 (2010).
[S9] L. Xiang, J. L. Palma, C. Bruot, V. Mujica, M. A. Ratner, N. Tao *Intermediate tunneling-hopping regime in DNA charge transport* Nature Chem. 2015, 20 221-226.
[S10] Y. Li, J. M. Artes, J. Hihath *Long-Range Charge Transport in Adenine-Stacked RNA:DNA Hybrids* Small 2016, 12, 432-47.
[S11] X. Yin, E. Wierzbinski, H. Lu, S. Bezer, A. R. de Leon, K. L. Davis, C. Achim, and D. H. Waldeck, A Three-Step Kinetic Model for Electrochemical Charge Transfer in the Hopping Regime J. Phys. Chem. A 118 (2014) 7579-7589.
[S12] C. H. Wohlgamuth, M. A. McWilliams, and J. D. Slinker DNA as a Molecular Wire: Distance and Sequence Dependence Anal. Chem. 2013, 85, 8634−8640
[S13] G. I. Livshits, A. Stern, D. Rotem, N. Borovok, G. Eidelshtein, A. Migliore, E. Penzo, S. J. Wind, R. Di Felice, S. S. Skourtis, J. C. Cuevas, L. Gurevich A. B. Kotlyar, and D. Porath *Long-range charge transport in single G-quadruplex DNA molecules* Nature Nanotech. 2014, 9 1040-1046.
[S14] C. M. Soukoulis, J. V. Jos e, E. N. Economou, and P. Sheng, Localization in One-Dimensional Disordered Systems in the Presence of an Electric Field*, Phys. Rev. Lett*. 50, 764-767 (1983).
[S15] P. W. Anderson, D. J. Thouless, E. Abrahams, and D. Fisher, New method for a scaling theory of localization, Phys. Rev. B 22, 3519 (1980).
[S16] J. Bellissard, A. Formoso, R. Lima, and D. Testard, Quasiperiodic interaction with a metal-insulator transition, Phys. Rev. B 26, 3024 (1982).
[S17] S. Datta, Electronic Transport in Mesoscopic Systems, Cambridge Studies in Semiconductor Physics and Microelectronic Engineering (Cambridge University Press, 1995).